J Elast (2010) 99: 179–201
DOI 10.1007/s10659-009-9239-8

Exact Solutions and Material Tailoring for Functionally Graded Hollow Circular Cylinders

G.J. Nie · R.C. Batra

Received: 7 August 2009 / Published online: 16 January 2010

Abstract We employ the Airy stress function to derive analytical solutions for plane strain static deformations of a functionally graded (FG) hollow circular cylinder with Young's modulus E and Poisson's ratio v taken to be functions of the radius r. For E_1 and v_1 power law functions of r, and for E_1 an exponential but v_1 an affine function of r, we derive explicit expressions for stresses and displacements. Here E_1 and v_1 are effective Young's modulus and Poisson's ratio appearing in the stress-strain relations. It is found that when exponents of the power law variations of E_1 and v_1 are equal then stresses in the cylinder are independent of v_1; however, displacements depend upon v_1. We have investigated deformations of a FG hollow cylinder with the outer surface loaded by pressure that varies with the angular position of a point, of a thin cylinder with pressure on the inner surface varying with the angular position, and of a cut circular cylinder with equal and opposite tangential tractions applied at the cut surfaces. When v_1 varies logarithmically through-the-thickness of a hollow cylinder, then the maximum radial stress, the maximum hoop stress and the maximum radial displacements are noticeably affected by values of v_1. Conversely, we find how E_1 and v_1 ought to vary with r in order to achieve desired distributions of a linear combination of the radial and the hoop stresses. It is found that for the hoop stress to be constant in the cylinder, E_1 and v_1 must be affine functions of r. For the in-plane shear stress to be uniform through the cylinder thickness, E_1 and v_1 must be functions of r^2. Exact solutions and optimal design parameters presented herein should serve as benchmarks for comparing approximate solutions derived through numerical algorithms.

Keywords Material tailoring · Airy stress function · Optimal design · Functionally graded cylinders · Poisson's ratio variations

Mathematics Subject Classification (2000) 74E·5 · 74B·5 · 45B·5

G.J. Nie
School of Aerospace Engineering and Applied Mechanics, Tongji University, Shanghai 200092, China

G.J. Nie · R.C. Batra (✉)
Department of Engineering Science and Mechanics, M/C 0219, Virginia Polytechnic Institute and State University, Blacksburg, VA 24061, USA
e-mail: rbatra@vt.edu

1 Introduction

Functionally graded materials (FGMs) generally have moduli continuously varying in one or more spatial directions and their use may optimize one or more functional characteristics of a structure, e.g., by using FGMs one can reduce stress concentration around a hole [1] in a plate and at interfaces between adjoining layers made of distinct materials [2]. Similarly material properties can be tailored to optimize the fundamental frequency of a laminated plate [3]. References [4–9] have discussed the mechanical performance of FG structures such as cylinders, spheres and plates used in aerospace, marine, and civil engineering fields.

From mathematics point of view FG structures are inhomogeneous bodies, and solutions for several problems involving inhomogeneous linear elastic materials can be found in Lekhnitskii's book [10]. One could potentially divide a FG plate into several thin perfectly bonded layers with different but constant material properties, e.g., see Timoshenko and Goodier's book [11] for composite cylinders. With an increase in the number of layers, the solution of the layered structure approaches that of a FG body. Even though Batra [12] used the finite element method to analyze axisymmetric finite deformations of a pressurized hollow cylinder composed of a FG Mooney-Rivlin material, his evaluation of material properties at integration points is equivalent to dividing the cylinder into several homogeneous thin cylinders each made of a homogeneous material. Pan and Roy [13] have used a similar technique coupled with the method of separation of variables and the expansion of unknowns in terms of the Fourier series in the circumferential direction to study plane strain static deformations of a FG isotropic elastic cylinder.

Horgan and Chan [14] have analyzed deformations of a FG cylinder composed of a compressible isotropic linear elastic material with Young's modulus E a power law function of the radius r and Poisson's ratio v constant. Tarn [15] has studied thermomechanical deformations of FG cylinders deformed in tension, torsion, shearing, and radial expansion due to pressure loading and temperature changes. Jabbari et al. [16] and Zimmerman and Lutz [17] have analyzed two-dimensional thermoelastic problems for hollow FG cylinders. Oral and Anlas [18] have computed stresses in a FG anisotropic cylinder. Shao and Ma [19] have studied three-dimensional thermo-elastic deformations of a FG cylindrical panel of finite length and subjected to nonuniform mechanical and steady-state thermal loads. Tarn and Chang [20] have analyzed the torsion of elastic circular bars of radially inhomogeneous, cylindrically orthotropic materials with emphasis on the end effects. Batra [21] has studied torsional deformations of a solid circular cylinder composed of an incompressible linear elastic isotropic material with the shear modulus varying in the axial direction.

Besides assuming that the elastic moduli vary according to a power-law function of r, some investigators have presumed that they are exponential functions of r. Based on the assumption that Poisson's ratio v is constant and Young's modulus E is an exponential function of r, Tutuncu [22], Chen and Lin [23], and Theotokoglou and Stampouloglou [24] have analyzed stresses and displacements in FG cylindrical pressure vessels.

The aforementioned works have presumed that v is constant but E varies. However, experimental measurements by Marur and Tippur [25] indicate that v also varies with the position in a FG material. Problems with both E and v varying with position have been studied in [26, 27]; e.g., Mohammadi and Dryden [26] assumed that v varies in the same way as E, and Li and Peng [27] analyzed axisymmetric deformations of a FG hollow cylinder or disk with arbitrarily varying material properties by expressing the radial displacement in terms of Legendre polynomials. Here we study both axisymmetric and non-axisymmetric problems for a FG cylinder with E and v independent functions of r.

We also investigate the material tailoring problem and find the spatial variation of material properties to achieve a desired stress distribution in a cylinder under prescribed boundary

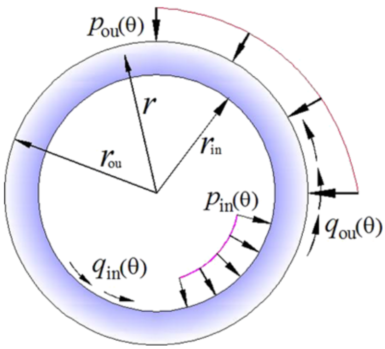

Fig. 1 Section of an infinitely long hollow circular cylinder

conditions. For plane strain axisymmetric deformations of a FG cylinder composed of an orthotropic material, Leissa and Vagins [1] assumed that all material moduli are proportional to each other and found their spatial variation to make either the hoop stress or the in-plane shear stress uniform in the cylinder. Here we do not assume that E and v are proportional to each other.

2 Problem Formulation

Consider an infinitely long hollow circular cylinder with inner radius r_{in}, and outer radius r_{ou}, subjected to pressures $p_{in}(\theta)$, $p_{ou}(\theta)$ and tangential tractions $q_{in}(\theta)$, $q_{ou}(\theta)$ on its inner and outer surfaces, as shown in Fig. 1. We assume that the cylinder is made of a linear elastic isotropic material with E and v varying only in the radial direction, and study its plane strain deformations. In the absence of body forces equations of equilibrium in cylindrical coordinates (r, θ) are

$$\begin{aligned} \frac{\partial \sigma_{rr}}{\partial r} + \frac{1}{r}\frac{\partial \sigma_{r\theta}}{\partial \theta} + \frac{\sigma_{rr} - \sigma_{\theta\theta}}{r} &= 0, \\ \frac{\partial \sigma_{r\theta}}{\partial r} + \frac{1}{r}\frac{\partial \sigma_{\theta\theta}}{\partial \theta} + \frac{2}{r}\sigma_{r\theta} &= 0, \end{aligned} \tag{1}$$

where σ_{rr}, $\sigma_{r\theta}$ and $\sigma_{\theta\theta}$ are stress components. The radial and the circumferential displacements, u_r and u_θ, are related to the strains ε_{rr}, $\varepsilon_{\theta\theta}$ and $\varepsilon_{r\theta}$ by

$$\varepsilon_{rr} = \frac{\partial u_r}{\partial r}, \qquad \varepsilon_{\theta\theta} = \frac{u_r}{r} + \frac{1}{r}\frac{\partial u_\theta}{\partial \theta}, \qquad \varepsilon_{r\theta} = \frac{1}{r}\frac{\partial u_r}{\partial \theta} + \frac{\partial u_\theta}{\partial r} - \frac{u_\theta}{r}. \tag{2}$$

The compatibility equation in terms of strains is

$$\frac{\partial^2 \varepsilon_{\theta\theta}}{\partial r^2} + \frac{1}{r^2}\frac{\partial^2 \varepsilon_{rr}}{\partial \theta^2} + \frac{2}{r}\frac{\partial \varepsilon_{\theta\theta}}{\partial r} - \frac{1}{r}\frac{\partial \varepsilon_{rr}}{\partial r} = \frac{1}{r}\frac{\partial^2 \varepsilon_{r\theta}}{\partial r \partial \theta} + \frac{1}{r^2}\frac{\partial \varepsilon_{r\theta}}{\partial \theta}. \tag{3}$$

Constitutive equations are

$$\varepsilon_{rr} = \frac{1}{E_1(r)}(\sigma_{rr} - v_1(r)\sigma_{\theta\theta}), \tag{4a}$$

$$\varepsilon_{\theta\theta} = \frac{1}{E_1(r)}(\sigma_{\theta\theta} - v_1(r)\sigma_{rr}), \tag{4b}$$

$$\varepsilon_{r\theta} = \frac{2(1+v_1(r))}{E_1(r)}\sigma_{r\theta}, \tag{4c}$$

where

$$E_1(r) = \frac{E(r)}{1-v^2(r)}, \qquad v_1(r) = \frac{v(r)}{1-v(r)}. \tag{4d}$$

Henceforth we call E_1 and v_1 effective Young's modulus and effective Poisson's ratio respectively. For $0 < v < 0.5$, v_1 varies from 0 to 1.

The pertinent boundary conditions on the inner and the outer surfaces of the cylinder are taken to be

$$\text{at} \quad r = r_{in}, \qquad \sigma_{rr}(r_{in},\theta) = -p_{in}(\theta), \qquad \sigma_{r\theta}(r_{in},\theta) = -q_{in}(\theta), \tag{5a}$$

$$\text{at} \quad r = r_{ou}, \qquad \sigma_{rr}(r_{ou},\theta) = -p_{ou}(\theta), \qquad \sigma_{r\theta}(r_{ou},\theta) = q_{ou}(\theta); \tag{5b}$$

or

$$\text{at} \quad r = r_{in}, \qquad u_r(r_{in},\theta) = 0, \qquad u_\theta(r_{in},\theta) = 0, \tag{5c}$$

$$\text{at} \quad r = r_{ou}, \qquad \sigma_{rr}(r_{ou},\theta) = -p_{ou}(\theta), \qquad \sigma_{r\theta}(r_{ou},\theta) = q_{ou}(\theta). \tag{5d}$$

For a traction boundary-value problem, prescribed surface tractions (5a), (5b) must have null resultant force and moment in order for the problem to have a solution. Equations (5c) imply that the inner surface of the cylinder is rigidly clamped.

3 Solution of the Problem

We introduce the Airy stress function in the form

$$\varphi(r,\theta) = \varphi_r(r)\varphi_\theta(\theta). \tag{6}$$

Thus stresses satisfying (1) are expressed as

$$\sigma_{rr} = \frac{\varphi_\theta(\theta)}{r}\frac{d\varphi_r(r)}{dr} + \frac{\varphi_r(r)}{r^2}\frac{d^2\varphi_\theta(\theta)}{d\theta^2}, \tag{7a}$$

$$\sigma_{\theta\theta} = \varphi_\theta(\theta)\frac{d^2\varphi_r(r)}{dr^2}, \tag{7b}$$

$$\sigma_{r\theta} = \frac{\varphi_r(r)}{r^2}\frac{d\varphi_\theta(\theta)}{d\theta} - \frac{1}{r}\frac{d\varphi_\theta(\theta)}{d\theta}\frac{d\varphi_r(r)}{dr}. \tag{7c}$$

Substitution for stresses from (7) into (4) and the result into (3) gives

$$\frac{d^4\varphi_\theta}{d\theta^4} + f_1(\varphi_r)\frac{d^2\varphi_\theta}{d\theta^2} + f_2(\varphi_r)\varphi_\theta = 0, \tag{8}$$

where

$$f_1(\phi_r) = 4 + \frac{2r^2}{\phi_r}\frac{d^2\phi_r}{dr^2} - \frac{2r}{\phi_r}\frac{d\phi_r}{dr} + \frac{1}{E_1(r)}\frac{dE_1(r)}{dr}\left[3r - \frac{2r^2}{\phi_r}\frac{d\phi_r}{dr} + 2r^2\frac{dv_1(r)}{dr}\right]$$

$$+\,v_1(r)r^2\left[\frac{1}{E_1(r)}\frac{d^2E_1(r)}{dr^2}-2\left(\frac{1}{E_1(r)}\frac{dE_1(r)}{dr}\right)^2\right]-r^2\frac{d^2v_1(r)}{dr^2}, \tag{9a}$$

$$\begin{aligned}f_2(\phi_r) &= \frac{r^4}{\phi_r}\frac{d^4\phi_r}{dr^4}+\frac{2r^3}{\phi_r}\frac{d^3\phi_r}{dr^3}-\frac{r^2}{\phi_r}\left(1+r\frac{dv_1(r)}{dr}\right)\frac{d^2\phi_r}{dr^2}+\frac{r}{\phi_r}\left(1-r^2\frac{d^2v_1(r)}{dr^2}\right)\frac{d\phi_r}{dr}\\ &\quad+\frac{1}{E_1(r)}\frac{dE_1(r)}{dr}\left[-\frac{2r^4}{\phi_r}\frac{d^3\phi_r}{dr^3}+\frac{(v_1-2)r^3}{\phi_r}\frac{d^2\phi_r}{dr^2}+\frac{r^2}{\phi_r}\frac{d\phi_r}{dr}+\frac{2r^3}{\phi_r}\frac{dv_1(r)}{dr}\frac{d\phi_r}{dr}\right]\\ &\quad-\left[\frac{1}{E_1(r)}\frac{d^2E_1(r)}{dr^2}-2\left(\frac{1}{E_1(r)}\frac{dE_1(r)}{dr}\right)^2\right]\left[\frac{r^4}{\phi_r}\frac{d^2\phi_r}{dr^2}-\frac{v_1(r)r^3}{\phi_r}\frac{d\phi_r}{dr}\right],\end{aligned} \tag{9b}$$

and we have tacitly assumed that $\varphi_r(r)\neq 0$, $\varphi_\theta(\theta)\neq 0$, $\frac{df_1(\varphi_r)}{dr}\neq 0$ and $E_1(r)\neq 0$.

Differentiation of both sides of (8) with respect to r gives

$$\frac{1}{\varphi_\theta}\frac{d^2\varphi_\theta}{d\theta^2}=-\frac{df_2(\varphi_r)}{dr}\bigg/\frac{df_1(\varphi_r)}{dr}=-\lambda^2, \tag{10a}$$

where λ is a constant. Thus for $\lambda\neq 0$ the expression for φ_θ is

$$\varphi_\theta=C_{11}\cos(\lambda\theta)+C_{12}\sin(\lambda\theta), \tag{10b}$$

and for $\lambda=0$ (10a) has the solution

$$\varphi_\theta=C_{21}\theta+C_{22}, \tag{10c}$$

where C_{11}, C_{12}, C_{21} and $C_{22}$are constants to be determined from boundary conditions. The constant λ is associated with the circumferential wave number. Substitution for φ_θ from (10) into (8) gives the following fourth-order ordinary differential equation with variable coefficients for the determination of function φ_r:

$$\lambda^4-\lambda^2 f_1(\varphi_r)+f_2(\varphi_r)=0. \tag{11}$$

Having found φ_r and φ_θ for different values of λ we get the following expression for the stress function $\varphi(r,\theta)$ from (6):

$$\varphi(r,\theta)=\sum_i\varphi_r(\lambda_i,r)\varphi_\theta(\lambda_i,\theta). \tag{12}$$

The corresponding stresses, strains, and displacements are derived from (7), (4) and (2). Provided that $E(r)>0$ and $-1<v(r)<0.5$, a unique solution of the boundary-value problem is obtained within a superimposed rigid body motion. For some boundary-value problems it may suffice to consider only one value of λ in (10b), (10c), while for others one may need to express the Airy stress function in terms of an infinite series. When all prescribed functions on the boundary vary as $\sin(k\theta)$ or $\cos(k\theta)$, it suffices to consider only one value of $\lambda=k$ in (10b). Constants appearing in (12) are found by satisfying boundary conditions in the sense of Fourier series.

3.1 Power-Law Variations of E_1 and v_1

We assume that the effective Young's modulus E_1 and the effective Poisson's ratio v_1 are given by

$$E_1(r)=E_0(r/r_{ou})^m, \tag{13a}$$

$$\upsilon_1(r) = \upsilon_0(r/r_{ou})^n, \tag{13b}$$

where E_0 and υ_0 are values, respectively, of E_1 and υ_1 at a point on the outer surface of the cylinder, and m and n are real numbers. Substitution from (13) into (9) and the result into (11) yields

$$\frac{d^4\varphi_r}{dr^4} + \frac{2(1-m)}{r}\frac{d^3\varphi_r}{dr^3} + z_3(r)\frac{d^2\varphi_r}{dr^2} + z_2(r)\frac{d\varphi_r}{dr} + z_1(r)\varphi_r = 0, \tag{14}$$

where

$$z_1(r) = r^{-4}(\lambda^2(\lambda^2 - 3m - 4) + \upsilon_0\lambda^2(m + m^2 - n - 2mn + n^2)r^n r_{ou}^{-n}),$$
$$z_2(r) = r^{-3}((m+1)(2\lambda^2 + 1) + \upsilon_0(n + 2mn - n^2 - m - m^2)r^n r_{ou}^{-n}),$$
$$z_3(r) = r^{-2}(m(m-1) - 2\lambda^2 - 1 - \upsilon_0(m-n)r^n r_{ou}^{-n}).$$

For $m = n$, in the expressions for z_1, z_2 and z_3 terms involving υ_0 are identically zero and the response of the FG solid is the same as that of the solid with $\upsilon_1 = 0 = \upsilon$. For this case, (14) reduces to the Cauchy-Euler form and has the solution

$$\varphi_r = \sum_{i=1}^{4} D_{0i} r^{s_i}, \tag{15a}$$

where constants $D_{01}, D_{02}, D_{03}, D_{04}$ and $D_{i1}, D_{i2}, D_{i3}, D_{i4} (i = 1, 2, \ldots)$ appearing below are determined from boundary conditions (5), and $s_i (i = 1, 2, 3, 4)$ is the root of the following equation:

$$s^4 - 2(m+2)s^3 + (4 - 2\lambda^2 + m^2 + 5m)s^2 + (m+2)(2\lambda^2 - m)s + \lambda^2(\lambda^2 - 4 - 3m) = 0.$$

For $m = n = 0$ and $\lambda = 0$, the solution of (14) is

$$\varphi_r = D_{11}\ln r + D_{12}r^2 + D_{13}r^2\ln r + D_{14}, \tag{15b}$$

the cylinder material is homogeneous and its deformations are axisymmetric. The stress function (15b) is the same as that given in [11]. For axisymmetric deformations (i.e., $\lambda = 0$) of an inhomogeneous cylinder and different values of m and n, e.g., $m = -2, n = 0$; $m \neq 0, m \neq -2, n = 0$; $m = 1, n = 1$; and $m = -1, n = -1$, solutions of (14), respectively, are

$$\varphi_r = D_{21}r^{-a_1} + D_{22}r^{a_1} + D_{23}\ln r + D_{24}, \tag{15c}$$
$$\varphi_r = D_{31}r^{a_2} + D_{32}r^{a_3} + D_{33}r^{2+m} + D_{34}, \tag{15d}$$
$$\varphi_r = D_{41}r^{a_5} + D_{42}r^{a_6} + D_{43}r^3 + D_{44}, \tag{15e}$$
$$\varphi_r = D_{51}r^{a_7} + D_{52}r^{a_8} + D_{53}r + D_{54}, \tag{15f}$$

where expressions for a_i $(i = 1, 2, \ldots, 8)$ are given in Appendix A.

For non-axisymmetric deformations of a homogeneous cylinder (i.e., $m = 0, n = 0$), analytical solutions for $\lambda = 1$ and $\lambda \neq 1$, respectively, are

$$\varphi_r = D_{61}r^{-1} + D_{62}r + D_{63}r\ln r + D_{64}r^3, \tag{15g}$$
$$\varphi_r = D_{71}r^{-\lambda} + D_{72}r^{2-\lambda} + D_{73}r^{\lambda} + D_{74}r^{2+\lambda}. \tag{15h}$$

For non-axisymmetric deformations of an inhomogeneous cylinder (i.e., $\lambda \neq 0$), and $m \neq 0, n = 0$; $m = 1, n = 1$; and $m = -1, n = -1$, the respective analytical solutions are

$$\varphi_r = \sum_{j=1}^{4} D_{8j} r^{b_j}, \tag{15i}$$

$$\varphi_r = \sum_{j=1}^{4} D_{9j} r^{c_j}, \tag{15j}$$

$$\varphi_r = \sum_{j=1}^{4} D_{10j} r^{d_j}, \tag{15k}$$

where expressions for b_i $(i = 1, 2, 3, 4)$, c_i $(i = 1, 2, 3, 4)$, and d_i $(i = 1, 2, 3, 4)$ are given in Appendix A. For $m \neq \pm 1, n \neq \pm 1$ and $\lambda \neq 0$, and other values of these three variables, (14) can be solved numerically.

The stress function is obtained by combining (10) and (15), and constants appearing in these equations are determined from boundary conditions (5). Arbitrary loads on the inner and the outer surfaces are expanded in Fourier series in θ, and boundary conditions are satisfied in the sense of Fourier series.

3.1.1 Axisymmetric Deformations of a FG Cylinder

For a homogeneous cylinder (i.e., for $m = 0, n = 0$) loaded by uniform tractions (i.e., $\lambda = 0$) on the inner and the outer surfaces expressions for stresses and displacements are given in many references, and hence are omitted. The remaining results in this subsection are for FG cylinders but for tractions with $\lambda = 0$.

For $m = -2, n = 0$, setting $C_{21} = 0$ in (10c) and substituting from it and (15c) into (7), we get the following for stresses in the FG cylinder.

$$\sigma_{rr} = -D_{21} a_1 r^{-2-a_1} + D_{22} a_1 r^{-2+a_1} + D_{23} r^{-2}, \tag{16a}$$

$$\sigma_{\theta\theta} = D_{21} a_1 (a_1 + 1) r^{-2-a_1} + D_{22} a_1 (a_1 - 1) r^{-2+a_1} - D_{23} r^{-2}, \tag{16b}$$

$$\sigma_{r\theta} = 0. \tag{16c}$$

Substitution for stresses from (16) and for E_1 and v_1 from (13) into (4) gives expressions for strains which upon integration give

$$u_r = \frac{1 + v_0}{E_0 r_{ou}^2} (D_{21}(2 + a_1) r^{1-a_1} - D_{22}(-2 + a_1) r^{1+a_1} + D_{23} r) + f(\theta), \tag{17a}$$

$$u_\theta = -\frac{2 D_{23}(1 + v_0) r\theta}{E_0 r_{ou}^2} - \int f(\theta) d\theta + f_r(r). \tag{17b}$$

The unknown functions $f(\theta)$ and $f_r(r)$ in (17) are determined by setting the shear strain equal to zero and requiring that the circumferential displacement is single-valued. For boundary conditions $p_{in}(\theta) = p_{in}$ and $p_{ou}(\theta) = p_{ou}$, we get the following expressions for stresses and displacements.

$$\sigma_{rr} = \frac{T_1 r^{a_1-2} + T_2 r^{-a_1-2}}{r_{in}^{2a_1} - r_{ou}^{2a_1}}, \qquad \sigma_{\theta\theta} = \frac{T_1(a_1 - 1) r^{a_1-2} - (a_1 + 1) T_2 r^{-a_1-2}}{r_{in}^{2a_1} - r_{ou}^{2a_1}},$$
$$\sigma_{r\theta} = 0, \tag{18}$$

$$u_r = \frac{T_3 r^{1+a_1} + T_4 r^{1-a_1}}{E_0 r_{ou}^2 (r_{in}^{2a_1} - r_{ou}^{2a_1})}, \qquad u_\theta = 0, \tag{19}$$

where expressions for T_i $(i = 1, 2, 3, 4)$ are given in Appendix B.

For $m \neq 0, m \neq -2, n = 0$, stresses and displacements are given below:

$$\sigma_{rr} = \frac{T_5 r^{a_2+a_4-2} + T_6 r^{a_2-2}}{r_{in}^{a_4} - r_{ou}^{a_4}}, \qquad \sigma_{\theta\theta} = \frac{T_5(a_4+m) r^{a_2+a_4-2} - T_6(a_4-m) r^{a_2-2}}{2(r_{in}^{a_4} - r_{ou}^{a_4})},$$
$$\sigma_{r\theta} = 0, \tag{20}$$

and

$$u_r = \frac{T_7 r^{a_2+a_4-m-1} + T_8 r^{a_2-m-1}}{2E_0(r_{in}^{a_4} - r_{ou}^{a_4})}, \qquad u_\theta = 0, \tag{21}$$

where expressions for T_i $(i = 5, 6, 7, 8)$ are given in Appendix B.

For $m = 1, n = 1$, stresses and displacements have the following expressions:

$$\sigma_{rr} = \frac{T_9 r^{-a_7} + T_{10} r^{-a_8}}{r_{in}^{\sqrt{5}} - r_{ou}^{\sqrt{5}}}, \qquad \sigma_{\theta\theta} = \frac{a_8 T_9 r^{-a_7} + a_7 T_{10} r^{-a_8}}{r_{in}^{\sqrt{5}} - r_{ou}^{\sqrt{5}}}, \qquad \sigma_{r\theta} = 0, \tag{22}$$

$$u_r = \frac{T_{11} r^{1-a_7} + T_{12} r^{-a_7} + T_{13} r^{1-a_8} + T_{14} r^{-a_8}}{E_0(r_{in}^{\sqrt{5}} - r_{ou}^{\sqrt{5}})}, \qquad u_\theta = 0, \tag{23}$$

where expressions for T_i $(i = 9, \ldots, 14)$ are given in Appendix B.

For $m = -1, n = -1$, we get the following for stresses and displacements:

$$\sigma_{rr} = \frac{T_{15} r^{-a_5} + T_{16} r^{-a_6}}{r_{in}^{\sqrt{5}} - r_{ou}^{\sqrt{5}}}, \qquad \sigma_{\theta\theta} = \frac{-a_7 T_{15} r^{-a_5} - a_8 T_{16} r^{-a_6}}{r_{in}^{\sqrt{5}} - r_{ou}^{\sqrt{5}}}, \qquad \sigma_{r\theta} = 0, \tag{24}$$

$$u_r = \frac{T_{17} r^{2-a_5} + T_{18} r^{1-a_5} + T_{19} r^{2-a_6} + T_{20} r^{1-a_6}}{E_0 r_{ou}(r_{in}^{\sqrt{5}} - r_{ou}^{\sqrt{5}})}, \qquad u_\theta = 0, \tag{25}$$

where expressions for T_i $(i = 15, \ldots, 20)$ are given in Appendix B.

3.1.2 FG Cylinder Deformed by Tangential Tractions on the Outer Surface

For a FG cylinder subjected to tangential tractions $q_{ou}(\theta) = q_{ou}$ on the outer surface with the inner surface rigidly clamped (i.e., $u_r = u_\theta = 0$ on $r = r_{in}$) deformations are axisymmetric. However, we proceed without making this assumption, and use the Airy stress function corresponding to $\lambda = 0$, and set $C_{22} = 0$ in (10c). For $m = n = 0$, substitution for the Airy stress function from (15b) and (10c) into (7) gives the following expressions for stresses in the cylinder.

$$\sigma_{rr} = (D_{11} r^{-2} + 2D_{12} + D_{13}(1 + 2\ln r))\theta, \tag{26a}$$

$$\sigma_{\theta\theta} = (-D_{11} r^{-2} + 2D_{12} + D_{13}(3 + 2\ln r))\theta, \tag{26b}$$

$$\sigma_{r\theta} = -D_{11}(1 - \ln r) r^{-2} - D_{12} - D_{13}(1 + \ln r) + D_{14} r^{-2}. \tag{26c}$$

From (26), (4) and (2) we get the following for displacements.

$$u_r = -\frac{\theta(D_{11}(1+v_0) + r^2(2D_{12}(v_0-1) + D_{13}(v_0+1)) + 2D_{13}(v_0-1)r^2 \ln r)}{E_0 r} + f(\theta), \tag{27a}$$

$$u_\theta = \frac{2D_{13} r \theta^2}{E_0} - \int f(\theta) d\theta + f_r(r). \tag{27b}$$

Equating the shear strain obtained from the constitutive relation (4) to that derived from the strain-displacement relation (2), we conclude that

$$f_r(r) = -\frac{D_{11}(1+v_0)\ln r}{E_0 r} - \frac{4D_{12} r \ln r}{E_0} - \frac{D_{13} r \ln r(1+v_0+2\ln r)}{E_0} - \frac{D_{14}(1+v_0)}{E_0 r} + D_{15} r, \tag{28a}$$

$$f(\theta) = D_{16}\sin(\theta) + D_{17}\cos(\theta). \tag{28b}$$

Constants $D_{11}, D_{12}, D_{13}, D_{14}, D_{15}, D_{16}$ and D_{17} are determined from boundary conditions (5b), (5c) on the inner and the outer surfaces of the cylinder and requiring that displacements be single-valued. Thus the following expressions for stresses and displacements are found.

$$\sigma_{rr} = 0, \qquad \sigma_{\theta\theta} = 0, \qquad \sigma_{r\theta} = \frac{q_{ou} r_{ou}^2}{r^2}, \tag{29}$$

$$u_r = 0, \tag{30a}$$

$$u_\theta = \frac{q_{ou} r_{ou}^2 (1+v_0)(r^2 - r_{in}^2)}{E_0 r_{in}^2 r}. \tag{30b}$$

Stresses given by (29) are universal in the sense that these equations hold for all materials and both elastic and inelastic deformations even though only infinitesimal elastic deformations are analyzed herein.

For $m \neq 0, n \neq 0$ (29) and (30a) hold and we give below only expressions for u_θ for different values of m and n considered in Sect. 3.1.1.

$$\text{For } m = -2, n = 0, \quad u_\theta = \frac{2q_{ou}(1+v_0) r \ln(r/r_{in})}{E_0}. \tag{31}$$

$$\text{For } m \neq 0, m \neq -2, n = 0, \quad u_\theta = \frac{2q_{ou} r_{ou}^{2+m}(1+v_0)(r^{2+m} - r_{in}^{2+m})}{E_0(2+m) r_{in}^{2+m} r^{1+m}}. \tag{32}$$

$$\text{For } m = 1, n = 1, \quad u_\theta = \frac{q_{ou} r_{ou}^2 (r_{in}^3(-2r_{ou} - 3v_0 r) + (2r_{ou} + 3v_0 r_{in}) r^3)}{3E_0 r_{in}^3 r^2}. \tag{33}$$

$$\text{For } m = -1, n = -1, \quad u_\theta = \frac{q_{ou} r_{ou}(r - r_{in})(2r_{in} r + (r + r_{in}) r_{ou} v_0)}{E_0 r_{in}^2 r}. \tag{34}$$

For a FG cylinder subjected to tangential traction $q_{ou}\sin(\lambda\theta)$ or $q_{ou}\cos(\lambda\theta)$ on the outer surface, we use the Airy stress functions (10b) and (15) to solve the problem. For example, we study deformations of a FG cylinder with $m = n = 1$ and the load $q_{ou}(\theta) = q_{ou}\cos(2\theta)$ applied on its outer surface. Recalling (7c) we take $\lambda = 2$ and $C_{11} = 0$ in (10b) and substitute from (10b) and (15j) into (7) to get the following expressions for stresses in the cylinder.

$$\sigma_{rr} = \sum_{j=1}^{4}(c_j - 4) D_{9j} r^{c_j - 2}\sin(2\theta), \qquad \sigma_{\theta\theta} = \sum_{j=1}^{4} c_j(c_j - 1) D_{9j} r^{c_j-2}\sin(2\theta), \tag{35a}$$

Fig. 2 Cross section of a FG semicircular cylinder clamped at the left edge

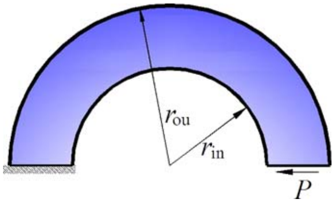

$$\sigma_{r\theta} = -2\sum_{j=1}^{4}(c_j - 1)D_{9j}r^{c_j-2}\cos(2\theta). \tag{35b}$$

Constants D_{9j} $(j = 1, 2, 3, 4)$ are determined from boundary conditions (5) on the inner and the outer surfaces of the cylinder. Knowing stresses, we can find strains and hence displacements; their lengthy expressions are omitted.

3.1.3 FG Semicircular Cylinder Deformed by a Tangential Force at One End

For a FG semicircular cylinder clamped at the left edge and loaded by a force P at the right edge, shown in Fig. 2, we use the Airy stress function given by (15) and (10b), and take $\lambda = 1$ and $C_{11} = 0$ to solve the problem. Recall that the bending moment at a horizontal cut plane is proportional to $\sin\theta$. For $m = 1, n = 0$, substitution from (10b) and (15i) into (7) gives the following expressions for stresses

$$\sigma_{rr} = ((b_1 - 1)D_{81}r^{b_1-2} + (b_2 - 1)D_{82}r^{b_2-2} + D_{84})\sin(\theta), \tag{36a}$$

$$\sigma_{\theta\theta} = (b_1(b_1 - 1)D_{81}r^{b_1-2} + b_2(b_2 - 1)D_{82}r^{b_2-2} + 2D_{84})\sin(\theta), \tag{36b}$$

$$\sigma_{r\theta} = -((b_1 - 1)D_{81}r^{b_1-2} + (b_2 - 1)D_{82}r^{b_2-2} + D_{84})\cos(\theta), \tag{36c}$$

where $b_1 = \frac{1}{2}(3 - \sqrt{21 - 4v_0})$, $b_2 = \frac{1}{2}(3 + \sqrt{21 - 4v_0})$.

From boundary conditions (5a), (5b) on the outer and the inner surfaces of semicircular cylinder, we get

$$(b_1 - 1)r_{in}^{b_1-2}D_{81} + (b_2 - 1)r_{in}^{b_2-2}D_{82} + r_{in}^2 D_{84} = 0, \tag{37a}$$

$$(b_1 - 1)r_{ou}^{b_1-2}D_{81} + (b_2 - 1)r_{ou}^{b_2-2}D_{82} + r_{ou}^2 D_{84} = 0. \tag{37b}$$

The boundary condition $\int_{r_{in}}^{r_{ou}} \sigma_{r\theta}dr = P$ on the surface $\theta = 0$ gives

$$(r_{in}^{b_1-1} - r_{ou}^{b_1-1})D_{81} + (r_{in}^{b_2-1} - r_{ou}^{b_2-1})D_{82} + (r_{in} - r_{ou})D_{84} = P, \tag{37c}$$

where we have assumed that b_1 and b_2 are unequal to 1. From (37), we can determine constants D_{81}, D_{82} and D_{84}. Then stresses and strains can be found. Displacements are determined by integrating the strain-displacement relation (2) and boundary conditions $u_r = u_\theta = 0$ at $\theta = \pi$.

3.2 Axisymmetric Deformations for E_1 and v_1 Given by Different Functions of r

We assume that

$$E_1(r) = E_0\exp(mr/r_{ou}), \qquad v_1(r) = v_0(1 + nr/r_{ou}). \tag{38}$$

Substituting for $E_1(r)$ and $v_1(r)$ from (38) into (4d) and solving the resulting equations, one can deduce the corresponding expressions for $E(r)$ and $v(r)$. Introducing a function ψ auxiliary to the Airy stress function φ, the hoop and the radial stresses are expressed as

$$\sigma_{rr} = \frac{\psi(r)}{r}, \qquad \sigma_{\theta\theta} = \frac{d\psi(r)}{dr}. \tag{39}$$

The compatibility equation for the axisymmetric problem in terms of strains is

$$\frac{d}{dr}(r\varepsilon_{\theta\theta}) - \varepsilon_{rr} = 0. \tag{40}$$

Substitution for stresses from (39) into (4) and the result into (40) yields

$$\frac{d^2\psi(r)}{dr^2} + \left(\frac{1}{r} - \frac{1}{E_1(r)}\frac{dE_1(r)}{dr}\right)\frac{d\psi(r)}{dr} + \left(\frac{v_1(r)}{rE_1(r)}\frac{dE_1(r)}{dr} - \frac{1}{r}\frac{dv_1(r)}{dr} - \frac{1}{r^2}\right)\psi(r) = 0. \tag{41}$$

Substituting for $E_1(r)$ and $v_1(r)$ from (38) into (41) and solving the resulting ordinary differential equation we get following expressions for the stress function ψ for different values of m and n.

$$\psi(r) = \exp(g_1)(C_1 U(g_2, 3, g_3) + C_2 L^2_{-g_2}(g_3)), \quad \text{when } m \neq 0, n \neq 0; \tag{42a}$$

$$\psi(r) = C_3 I_2(2\sqrt{nv_0 r/r_{ou}}) + C_4 K_2(2\sqrt{nv_0 r/r_{ou}}), \quad \text{when } m = 0, n \neq 0; \tag{42b}$$

$$\psi(r) = r(C_5 U(1 - v_0, 3, mr/r_{ou}) + C_6 L^2_{v_0 - 1}(mr/r_{ou})), \quad \text{when } m \neq 0, n = 0. \tag{42c}$$

Constants C_1, C_2, C_3, C_4, C_5 and C_6 in (42) are determined by boundary conditions (5), and

$$U(a, b, z) = 1/\Gamma(a) \int_0^\infty e^{-zt} t^{a-1} (1+t)^{b-a-1} dt,$$

is the confluent hypergeometric function, $\Gamma(a)$ the Euler gamma function, $L^a_n(x)$ the generalized Laguerre polynomial, $I_n(z)$ and $K_n(z)$ the modified Bessel functions of the first and the second kind, respectively, and

$$g_1 = \frac{mr - r\sqrt{m(m - 4nv_0)} + 2r_{ou}\ln r}{2r_{ou}},$$

$$g_2 = -\frac{m(1 + 2v_0) - 2nv_0 - 3\sqrt{m(m - 4nv_0)}}{2\sqrt{m(m - 4nv_0)}},$$

$$g_3 = \frac{r\sqrt{m(m - 4nv_0)}}{r_{ou}}.$$

Substitution from (42) into (39) gives stresses; strains and displacements can then be computed. Constants appearing in these equations are determined from the boundary conditions.

For $E_1 =$ constant (i.e., $m = 0$ in (38)) but v_1 given by

$$v_1(r) = v_{in} + (v_{ou} - v_{in})\frac{\ln(r/r_{in})}{\ln(r_{ou}/r_{in})}, \tag{43}$$

we get the following expression for the stress function ψ

$$\psi(r) = C_7 r^{s_1} + C_8 r^{-s_1}, \tag{44}$$

where v_{in} and v_{ou} are values of v_1 on the inner and the outer surfaces of the cylinder, respectively, $s_1 = \sqrt{1 + \frac{v_{ou} - v_{in}}{\ln(r_{ou}/r_{in})}}$. Constants C_7 and C_8 in (44) are determined by boundary conditions (5). Thus stresses, strains and displacements can be computed. Equation (43) for the effective Poisson's ratio is the same as (35) of [26].

4 Material Tailoring for Axisymmetric Deformations of the Cylinder

We now find the variation in the radial direction of Young's modulus and Poisson's ratio that will give the following distribution of the radial and the hoop stresses:

$$k\sigma_{rr} + \sigma_{\theta\theta} = C_0 r^{\beta}, \tag{45}$$

where k and β are known constants, and constant C_0 is related to pressures applied on the inner and the outer surfaces as well as the inner and the outer radii of the hollow cylinder.

Substitution for stresses from (39) into (45), and integration of the resulting equation gives

$$\psi(r) = \frac{C_0 r^{\beta+1}}{\beta + k + 1} + D_0 r^{-k}, \quad \text{when } k + \beta \neq -1. \tag{46}$$

We determine constants C_0 and D_0 from boundary conditions (5a), (5b) and thus obtain the following expressions for the stress function for different values of k and β.

$$\psi(r) = \frac{r^{-k}(p_{ou} r_{ou}^{k+1}(r^{k+\beta+1} - r_{in}^{k+\beta+1}) - p_{in} r_{in}^{k+1}(r^{k+\beta+1} - r_{ou}^{k+\beta+1}))}{r_{in}^{k+\beta+1} - r_{ou}^{k+\beta+1}},$$
$$\text{when } k + \beta \neq -1; \tag{47a}$$

$$\psi(r) = \frac{r((p_{ou} - p_{in})\ln r - p_{ou}\ln r_{in} + p_{in}\ln r_{ou})}{\ln(r_{in}/r_{ou})}, \quad \text{when } k = -1 \text{ and } \beta = 0; \tag{47b}$$

$$\psi(r) = \frac{(p_{in} r_{in} - p_{ou} r_{ou})\ln r + p_{ou} r_{ou}\ln r_{in} - p_{in} r_{in}\ln r_{ou}}{\ln(r_{ou}/r_{in})},$$
$$\text{when } k = 0 \text{ and } \beta = -1; \tag{47c}$$

$$\psi(r) = \frac{(p_{in} r_{in}^2 - p_{ou} r_{ou}^2)\ln r + p_{ou} r_{ou}^2\ln r_{in} - p_{in} r_{in}^2\ln r_{ou}}{r\ln(r_{ou}/r_{in})},$$
$$\text{when } k = 1 \text{ and } \beta = -2. \tag{47d}$$

4.1 Uniform Hoop Stress

For the hoop stress to be constant in the cylinder, we set $k = 0$ and $\beta = 0$ in (47a) and substitute for ψ in (41) to get

$$\frac{r(p_{in} r_{in} - p_{ou} r_{ou})}{E_1(r)}\frac{dE_1(r)}{dr} + \frac{r(p_{ou} r_{ou} - p_{in} r_{in}) + r_{in} r_{ou}(p_{in} - p_{ou})}{E_1(r)}\frac{dE_1(r)}{dr} v_1(r)$$
$$+ (r(p_{in} r_{in} - p_{ou} r_{ou}) + r_{in} r_{ou}(p_{ou} - p_{in}))\frac{dv_1(r)}{dr} + \frac{p_{ou} r_{ou} r_{in} - p_{in} r_{in} r_{ou}}{r} = 0. \tag{48}$$

We thus have one ordinary differential equation for two unknown functions. We assume the spatial variation of one of these functions, and solve (48) for the other function. For $v_1(r) = v_0$, where v_0 is a constant, (48) has the solution

$$E_1(r) = E_0 \exp\left(\frac{\ln(r/r_{ou}) + h_1 - h_2(r)}{v_0}\right), \tag{49}$$

where E_0 is a constant, and

$$h_1 = \ln(p_{in} r_{in} r_{ou} + p_{ou} r_{ou}(r_{ou}(v_0 - 1) - r_{in} v_0)),$$
$$h_2(r) = \ln(p_{ou} r_{ou}(r(v_0 - 1) - r_{in} v_0) + p_{in} r_{in}(r(1 - v_0) + r_{ou} v_0)).$$

For v_1 given by (13b) with n different from 0, the solution of (48) is

$$E_1(r) = E_{1in} \exp\left[\int_{r_{in}}^{r} f(x)dx\right], \tag{50}$$

where E_{1in} equals the value of E_1 at a point on the inner surface of the cylinder, and

$$f(x) = \frac{f_1(x)}{f_2(x)},$$
$$f_1(x) = (p_{in} - p_{ou}) r_{in} r_{ou} (r_{ou}^n + n v_0 x^n) - n(p_{in} r_{in} - p_{ou} r_{ou}) v_0 x^{n+1},$$
$$f_2(x) = x^2 (p_{in} r_{in} - p_{ou} r_{ou})(r_{ou}^n - v_0 x^n) + (p_{in} - p_{ou}) r_{in} r_{ou} v_0 x^{n+1},$$

and $f_2(r)$ is assumed not to vanish anywhere in the cylinder. It is difficult to evaluate in closed-form the integral in (50); however, one can evaluate it numerically.

For the function $E_1(r)$ given by (13a), (48) gives

$$v_1(r) = \frac{(v_0 - S_1 - S_2) r^m}{r_{ou}^m} + S_3(r) + S_4(r), \quad \text{when } m \neq 0 \text{ and } m \neq 1; \tag{51a}$$
$$v_1(r) = v_0 - \ln(r/r_{ou}) + \ln S_5(r), \quad \text{when } m = 0; \tag{51b}$$
$$v_1(r) = 1 + \frac{(v_0 - 1) r}{r_{ou}}, \quad \text{when } m = 1; \tag{51c}$$

where

$$S_1 = \frac{m(p_{ou} r_{ou} - p_{in} r_{in})\, {}_2F_1(1 - m, 1, 2 - m, y_1)}{(m - 1)(p_{in} - p_{ou}) r_{in}}, \qquad S_2 = \frac{{}_2F_1(-m, 1, 1 - m, y_1)}{m},$$
$$S_3(r) = \frac{mr(p_{ou} r_{ou} - p_{in} r_{in})\, {}_2F_1(1 - m, 1, 2 - m, y_2(r))}{(m - 1)(p_{in} - p_{ou}) r_{in} r_{ou}},$$
$$S_4(r) = \frac{{}_2F_1(-m, 1, 1 - m, y_2(r))}{m},$$
$$S_5(r) = \frac{p_{in} r_{in}(r - r_{ou})}{p_{ou} r_{ou}(r_{in} - r_{ou})} + \frac{r_{in} - r}{r_{in} - r_{ou}}, \qquad y_1 = \frac{p_{in} r_{in} - p_{ou} r_{ou}}{(p_{in} - p_{ou}) r_{in}},$$
$$y_2(r) = \frac{(p_{in} r_{in} - p_{ou} r_{ou}) r}{(p_{in} - p_{ou}) r_{in} r_{ou}},$$

and the hypergeometric function ${}_2F_1(a,b,c,z)$ has the series expansion

$$ {}_2F_1(a,b,c,z)=\sum_{k=0}^{\infty}((a)_k(b)_k/(c)_k)z^k/k!. $$

We thus have two combinations of $E_1(r)$ and $v_1(r)$ that give constant hoop stress in the cylinder. The corresponding radial and hoop stresses are given by

$$ \sigma_{rr}=\frac{p_{ou}r_{ou}(r-r_{in})+p_{in}r_{in}(r_{ou}-r)}{r(r_{in}-r_{ou})}, \tag{52a} $$

$$ \sigma_{\theta\theta}=\frac{p_{in}r_{in}-p_{ou}r_{ou}}{r_{ou}-r_{in}}. \tag{52b} $$

The hoop stress identically vanishes if $p_{in}r_{in}=p_{ou}r_{ou}$, and it is tensile for $p_{in}r_{in}>p_{ou}r_{ou}$ and compressive otherwise. The expression (52b) of the hoop stress is the same as (29) in [28] where the cylinder material is assumed to be incompressible.

4.2 Uniform In-Plane Shear Stress

For the in-plane shear stress to be uniform in the cylinder, i.e., $k=-1$ and $\beta=0$ in (47), we first consider the case of $v_1(r)=v_0$. Substitution for the stress function from (47b) into (41), and integrating the resulting equation, we get

$$ \begin{aligned} E_1(r)={}&E_0((p_{ou}-p_{in})(1-(v_0-1)\ln r)+(v_0-1)(p_{ou}\ln r_{in}-p_{in}\ln r_{ou}))^{\frac{2}{1-v_0}}\\ &\times(p_{ou}-p_{in}+p_{ou}(v_0-1)(\ln r_{in}-\ln r_{ou}))^{\frac{2}{v_0-1}}. \end{aligned} \tag{53} $$

For $p_{ou}=0$, this result agrees with (27) of Leissa and Vagins [1]. Note that through-the-thickness variation of E_1 depends upon the cylinder geometry and uniform pressures applied on its inner and outer surfaces.

For $E_1(r)$ given by (13a), we get

$$ v_1(r)=1+\left(\frac{r}{r_{ou}}\right)^m\left((v_0-1)+(m-2)\left(\frac{r_{in}}{r_{ou}}\right)^{\frac{mp_{ou}}{p_{in}-p_{ou}}}(\mathrm{Ei}(y_3)-\mathrm{Ei}(y_4(r)))\right), $$
$$ \text{when } m\neq 0; \tag{54a} $$

$$ v_1(r)=v_0-2\ln(p_{ou}(\ln r_{in}-\ln r_{ou}))+2\ln((p_{in}-p_{ou})\ln r+p_{ou}\ln r_{in}-p_{in}\ln r_{ou}), $$
$$ \text{when } m=0; \tag{54b} $$

where $\mathrm{Ei}(z)=-\int_{-z}^{\infty}\frac{e^{-t}}{t}dt$ is the exponential integration function, and

$$ y_3=\frac{mp_{ou}(\ln r_{ou}-\ln r_{in})}{p_{in}-p_{ou}},\qquad y_4(r)=-m\ln r+\frac{m(p_{ou}\ln r_{in}-p_{in}\ln r_{ou})}{p_{ou}-p_{in}}. $$

For $m=2$, (54a) gives

$$ v_1(r)=1+\frac{(v_0-1)r^2}{r_{ou}^2}. \tag{54c} $$

That is $v_1(r)$ is independent of pressures applied on the inner and the outer surfaces of the cylinder. For this case, stresses are given by

$$\sigma_{rr} = \frac{(p_{ou} - p_{in})\ln r - p_{ou}\ln r_{in} + p_{in}\ln r_{ou}}{\ln r_{in} - \ln r_{ou}}, \tag{55a}$$

$$\sigma_{\theta\theta} = \frac{(p_{ou} - p_{in})(1 + \ln r) - p_{ou}\ln r_{in} + p_{in}\ln r_{ou}}{\ln r_{in} - \ln r_{ou}}. \tag{55b}$$

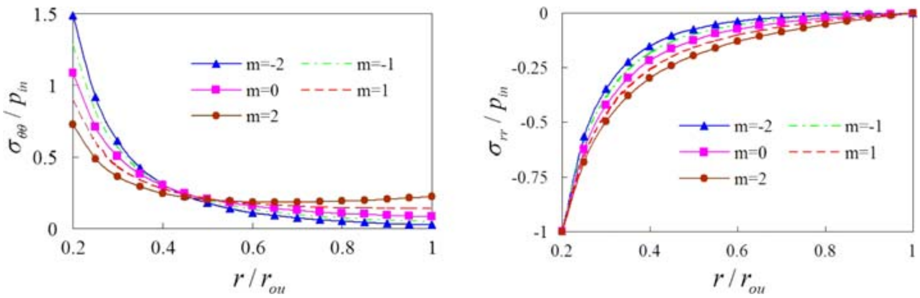

(a) hoop stress (b) radial stress

Fig. 3 Through-the-thickness variation of (**a**) the hoop stress, (**b**) the radial stress in a cylinder for $n = 0$ and different values of m

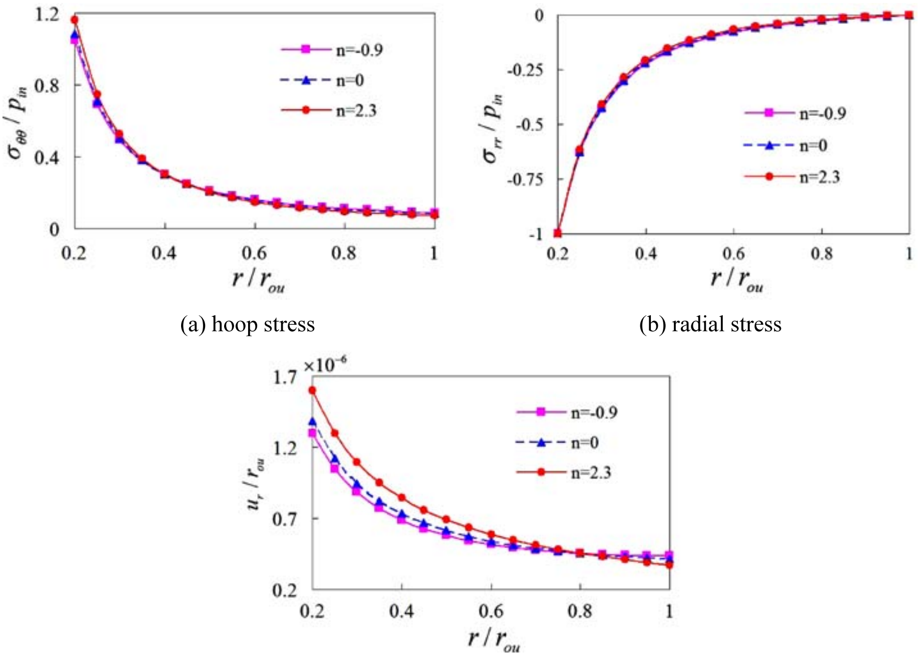

(a) hoop stress (b) radial stress

(c) radial displacement

Fig. 4 Through-the-thickness variation of (**a**) the hoop stress, (**b**) the radial stress, and (**c**) the radial displacement in a cylinder for $m = 0$ and different values of n

Spatial variations of E and ν corresponding to E_1 and ν_1 found above are deduced from (4d).

5 Numerical Examples

5.1 Axisymmetric Problem

Example 1 We analyze deformations of a cylinder with $r_{in} = 0.2$ cm, $r_{ou} = 1.0$ cm, $p_{in} = 1.0$ MPa, $p_{ou} = 0.0$, and in (38) $E_0 = 2 \times 10^5$ MPa, $\upsilon_0 = 0.3, n = 0$. For different values of m we have plotted in Fig. 3 the through-the-thickness variation of stresses. For the same parameters, stresses and radial displacement are plotted in Figs. 4 and 5 for $m = 0, 0.5$ and different values of n. For $n = -0.9$, ν_1 varies affinely from 0.246 at a point on the inner surface to 0.03 at a point on the outer surface. When $n = 2.3$, values of ν_1 on the inner and the outer surfaces equal 0.438 and 0.99 respectively. Through-the-thickness variations of the hoop stress plotted in Fig. 3 suggest that the hoop stress is nearly independent of the value of m at the point $r = \sim 0.45 = \sim\sqrt{r_{in}r_{ou}}$. At a fixed value of r, the two stresses continuously depend upon m. Stresses plotted in Figs. 4 and 5 are virtually independent of the value of n; thus the assumption of constant effective Poisson's ratio does not introduce any noticeable error in stresses. However, the effect of the variation of Poisson's ratio on the radial displacement is larger than that on stresses. The difference in the radial displacements of a point on the inner surface for $n = 2.3$ and $n = 0$ in Figs. 4(c) and 5(c) is about 16%. We note

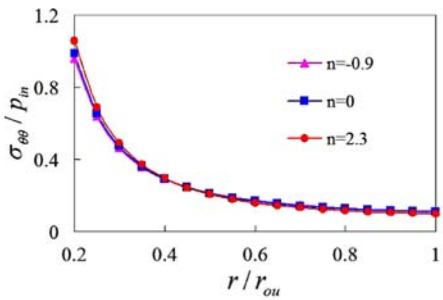

(a) hoop stress

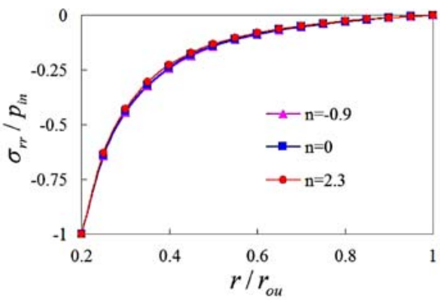

(b) radial stress

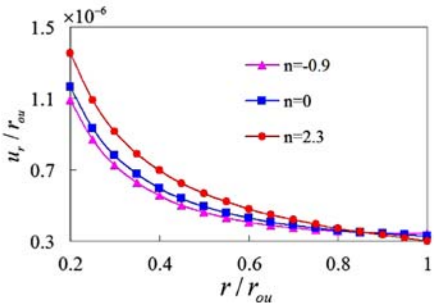

(c) radial displacement

Fig. 5 Through-the-thickness variation of (**a**) the hoop stress, (**b**) the radial stress, and (**c**) the radial displacement in a cylinder for $m = 0.5$ and different values of n

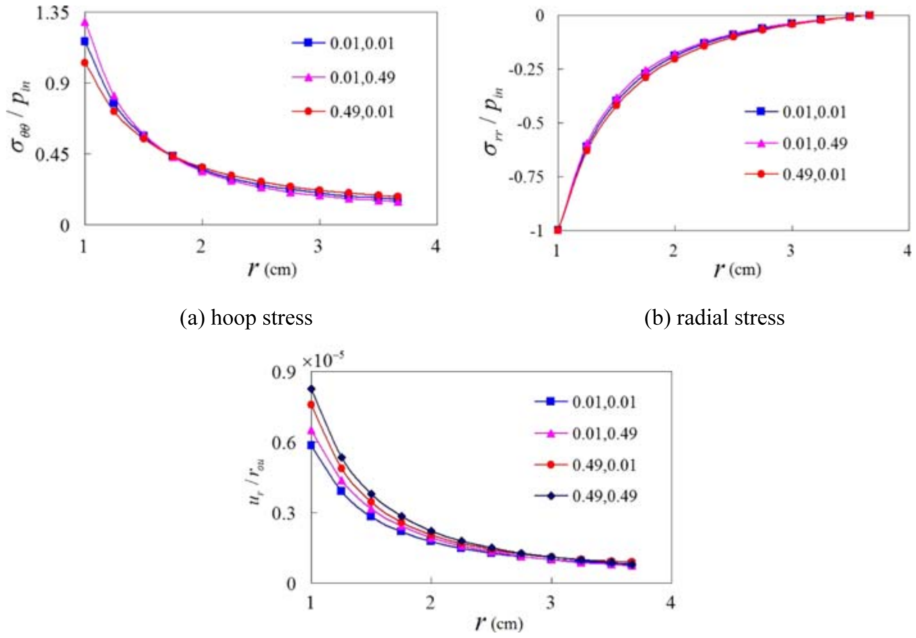

(a) hoop stress

(b) radial stress

(c) radial displacement

Fig. 6 Through-the-thickness variation of (**a**) the hoop stress, (**b**) the radial stress, and (**c**) the radial displacement in a cylinder for $m = 0$ in (13) and different values of v_0 and v_1 given in (43)

that for the problem studied in [26] the maximum hoop stress and the radial displacement in a pipe changed by ∼2% and ∼15%, respectively, when Young's modulus was held constant but Poisson's ratio was varied through the cylinder thickness according to (43) by a factor of 2.

Example 2 We investigate the effect of Poisson's ratio v_1 on stresses and displacements in the cylinder with v_1 given by (43) and constant Young's modulus $E_1 = 2 \times 10^5$ MPa. We take $r_{in} = 1.0$ cm, $r_{ou} = 3.669$ cm, $p_{in} = 1.0$ MPa, $p_{ou} = 0.0$, and compute results for $v_{in} = 0.01$, $v_{ou} = 0.49$, and $v_{in} = 0.49$, $v_{ou} = 0.01$ in (43). Through-the-thickness variations of stresses and the radial displacement for $(v_{in}, v_{ou}) = (0.01, 0.01)$, $(0.01, 0.49)$ and (0.49, 0.01) are depicted in Fig. 6. It is observed from Fig. 6(a) that the hoop stress is nearly independent of the variation of v_1 at the point $r = \sim 1.70 = \sim\sqrt{r_{in} r_{ou}}$. The maximum differences, ∼13% in the hoop stress, and ∼10% in the radial stress occur at points in the cylinder interior. The maximum radial displacement of a point on the inner surface for the three variations of v_1 is ∼30%. Thus the variation of Poisson's ratio with the radius noticeably affects the radial displacement of a point, and the maximum stresses induced in the cylinder.

5.2 Non-axisymmetric Deformations

Example 3 For the cylinder geometry considered in Example 1, E_1 and v_1 given by (13) with $m = 1, n = 1$, $E_0 = 2 \times 10^5$ MPa, $v_0 = 0.3$, $p_{in} = 0$, and $p_{ou} = 1.0$ MPa, $1.0 \times \cos(2\theta)$ MPa, $1.0 \times \cos(4\theta)$ MPa, we have plotted in Fig. 7 through-the-thickness variations of the radial

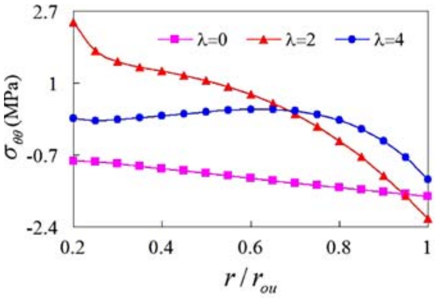

(a) hoop stress

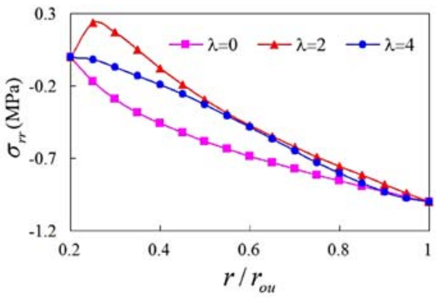

(b) radial stress

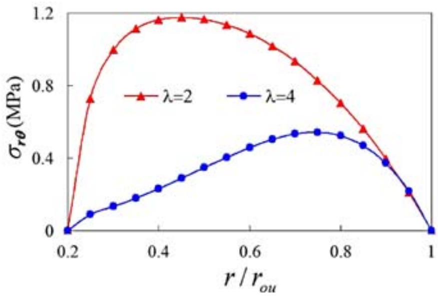

(c) shear stress

Fig. 7 Through-the-thickness variation of (**a**) the hoop stress, (**b**) the radial stress, (**c**) the shear stress in a cylinder for $m = 1$ and $n = 1$

and the hoop stresses. Results for these three pressure variations are obtained by considering only one term in (10b) and (10c) with $\lambda = 0, 2$ and 4 for $p_{ou} = 1.0$, $\cos(2\theta)$ and $\cos(4\theta)$ MPa, respectively. It is evident that the stress distribution for the non-axisymmetric pressure distribution is quite different from that for the axisymmetric problem even though the peak value of the applied pressure is the same. The maximum magnitudes of the hoop stress, the radial stress and the shear stress strongly depend upon the wave number of the pressure distribution on the outer surface of the cylinder. The maximum shear stress for $\lambda = 2$ is more than twice of that for $\lambda = 4$ and they occur at different points in the cylinder. Note that the radial stress at a point in the cylinder interior is tensile when $\lambda = 2$ but is compressive for $\lambda = 0$ and 4.

Example 4 For $r_{in}/r_{ou} = 0.95$, $p_{\mathrm{in}} = 1.0 \times \cos(\lambda\theta)$ MPa, $p_{\mathrm{ou}} = 0$, $E_0 = 2 \times 10^5$ MPa, $\upsilon_0 = 0.3$, $\lambda = 12, 20$ and the exponents $m = -2, 0, 2$ and $n = 0$ in (13), we have plotted in Fig. 8 through-the-thickness variations of the hoop stress and the shear stress to delineate effects of the non-axisymmetric pressure distribution on stresses in a thin FG cylinder. We note from Fig. 8 that the maximum hoop stress and the maximum shear stress strongly depend upon the circumferential wave number of the applied pressure but are unaffected by the gradation of the material properties. With an increase in the circumferential wave number from 12 to 20, the maximum hoop stress decreases from 16 to 6 MPa and the maximum shear stress from 2.3 to 1.4 MPa. The variation of the hoop stress from negative values on the inner surface to positive values on the outer surface of the same magnitude suggests that bending rather than stretching deformations are dominant in each one of the angular segments of

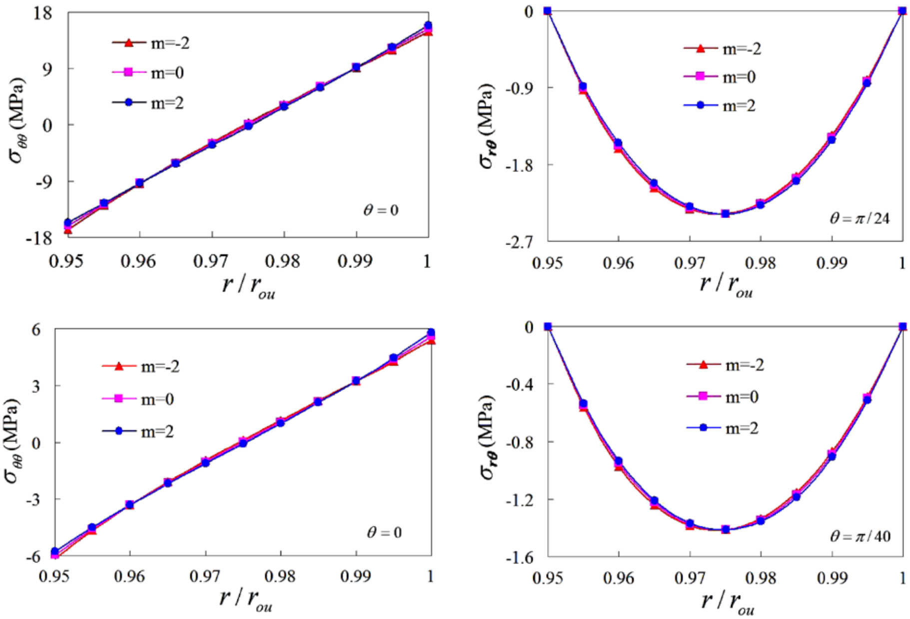

Fig. 8 For $\lambda = 12$ (*top*) and $\lambda = 20$ (*bottom*), $r_{in}/r_{ou} = 0.95$, through-the-thickness distributions of the hoop and the shear stresses in the cylinder

length $2\pi/\lambda$. For a uniformly loaded simply supported beam, the maximum axial stress is proportional to the square of the beam length. Thus for pure bending of the segment of thin cylinder between two cusps of the applied pressure, the maximum hoop stress for $\lambda = 20$ should be 36% of that for $\lambda = 12$ which is not too different from the 37.5% obtained here. A similar result was obtained in [29] for a FG cylinder composed of an incompressible linear elastic material.

Example 5 We study deformations of a semicircular cylinder clamped at the left edge and loaded by a tangential force P on the right edge as shown in Fig. 2. For $r_{in}/r_{ou} = 0.6$, $r_{ou} = 1$ cm, $P = 1$ N/cm, E_1 and v_1 given by (13) with $E_0 = 2 \times 10^5$ MPa, $v_0 = 0.3$, $n = 0$ and different values of m, through-the-thickness variations of the stresses are exhibited in Fig. 9. Results plotted in Fig. 9 reveal that the hoop stress and the shear stress depend continuously upon the material gradation index m. For $m = 1$, the hoop stress varies affinely with the radius.

5.3 Material Tailoring

For the cylinder with $r_{in}/r_{ou} = 0.6$, we have plotted in Fig. 10a through-the-thickness variations of $E_1(r)$ and $v_1(r)$ in order for the hoop stress to be constant. These results evince that both $E_1(r)$ and $v_1(r)$ must be affine functions of r in order to have constant hoop stress in the cylinder. Using (4d), the corresponding through-the-thickness variations of $E(r)$ and $v(r)$ are plotted in Fig. 10b, and are also nearly affine functions of r.

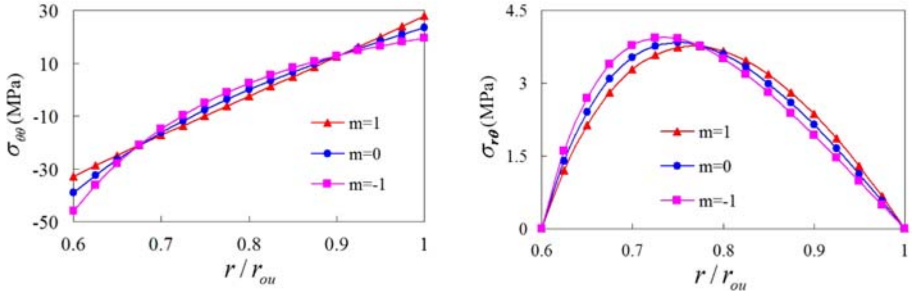

(a) the hoop stress (b) the shear stress

Fig. 9 For $r_{in}/r_{ou} = 0.6$, through-the-thickness distributions of (**a**) the hoop stress on the radial line $\theta = \pi/2$, and (**b**) the shear stress on the radial line $\theta = 0$ in a semicircular cylinder

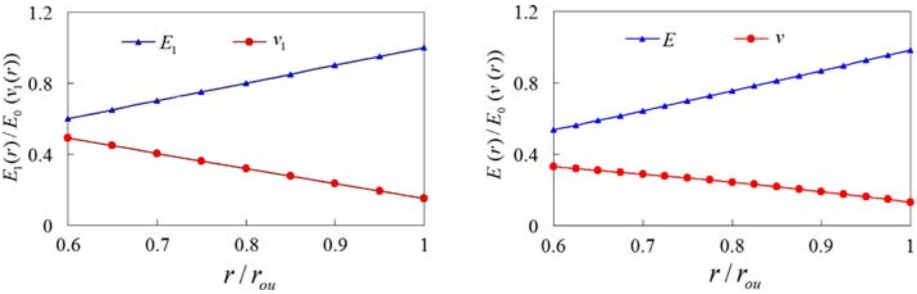

(a) E_1 and v_1 (b) E and v

Fig. 10 For constant hoop stress, through-the-thickness variations of (**a**) the effective Young's modulus and the effective Poisson's ratio, and (**b**) Young's modulus and Poisson's ratio

6 Remarks

Equations (4a)–(4c) with E_1 and υ_1 replaced, respectively, by E and υ are valid for plane stress deformations of FG linear elastic materials. Thus the analysis presented above applies to thin FG disks with boundary conditions (5) for which a plane stress state of deformation is a reasonable approximation. For a cylinder of length comparable to its outer diameter, one needs to solve three-dimensional problems.

Nonaxisymmetric deformations of FG cylinders made of incompressible linear elastic materials are analyzed in [29–31], and nonlinear axisymmetric deformations of FG cylinders are studied in [32–34].

7 Conclusions

We have analytically studied plane strain static deformations of a functionally graded hollow cylinder under both axisymmetric and non-axisymmetric loads applied to its inner and outer surfaces. The problem is solved by expressing the Airy stress function as the product of two functions—one of radius r and the other of the angular position θ. Exact solutions are given when the effective Young's modulus E_1 and the effective Poisson's ratio υ_1 are either power law functions of r, or when E_1 is an exponential and υ_1 an affine function of r.

Results for example problems including uniform and non-uniform pressure distributions on the inner and the outer surfaces are provided. It is found that the effect of the variation of Poisson's ratio on the radial displacement is considerably more (∼30%) than that (∼13%) on stresses. Stresses induced in the cylinder by non-uniform pressures applied on the outer surface noticeably differ both in magnitude and in sign from those induced by a uniform pressure of magnitude equal to the peak non-uniform pressure. For a thin cylinder loaded by the pressure proportional to $\cos(20\theta)$ on the inner surface, the cylinder length between two adjacent cusps of the cosine wave deforms due to bending rather than stretching of the material and the hoop stresses on the inner and the outer surfaces are equal and opposite of each other.

We have also analyzed the material tailoring problem in which through-the-thickness variations of Young's modulus and Poisson's ratio are found so that a linear combination of the radial and the hoop stresses has the desired through-the-thickness variation in the cylinder. For the hoop stress to be constant in the cylinder, it is found that E_1 and υ_1 must be affine functions of r. In order to achieve uniform in-plane shear stress through the cylinder thickness, E_1 and υ_1 must be functions of r^2.

Exact solutions presented here can serve as benchmarks for establishing the accuracy of the approximate solutions obtained numerically. The material tailoring results provide challenges to material scientists and engineers regarding how to design such composites.

Acknowledgements This work was supported by the Office of Naval Research Grant N00014-98-06-1-0567 to Virginia Polytechnic Institute and State University with Dr. Y.D.S. Rajapakse as the program manager. Views expressed herein are those of authors, and neither of the funding agencies nor of their institutions. Authors are indebted to an anonymous reviewer for useful suggestions that helped improve upon the presentation of the work.

Appendix A

Expressions for constants a_i $(i = 1, 2, \ldots, 8)$, b_i $(i = 1, 2, 3, 4)$, $c_i (i = 1, 2, 3, 4)$ and d_i $(i = 1, 2, 3, 4)$ appearing in (15) are given below.

$$a_1 = \sqrt{2(1+\upsilon_0)}, \qquad a_2 = 1 + \frac{1}{2}(m - a_4), \qquad a_3 = 1 + \frac{1}{2}(m + a_4),$$

$$a_4 = \sqrt{4 + m^2 - 4m\upsilon_0},$$

$$a_5 = \frac{3-\sqrt{5}}{2}, \qquad a_6 = \frac{3+\sqrt{5}}{2}, \qquad a_7 = \frac{1-\sqrt{5}}{2}, \qquad a_8 = \frac{1+\sqrt{5}}{2},$$

$$b_1 = \frac{1}{2}(2 + m - B_5), \qquad b_2 = \frac{1}{2}(2 + m + B_5), \qquad b_3 = \frac{1}{2}(2 + m - B_6),$$

$$b_4 = \frac{1}{2}(2 + m + B_6),$$

$$c_1 = \frac{1}{2}(3 - C_5), \qquad c_2 = \frac{1}{2}(3 + C_5), \qquad c_3 = \frac{1}{2}(3 - C_6), \qquad c_4 = \frac{1}{2}(3 + C_6),$$

$$d_1 = \frac{1}{2}(1 - D_5), \qquad d_2 = \frac{1}{2}(1 + D_5), \qquad d_3 = \frac{1}{2}(1 - D_6), \qquad d_4 = \frac{1}{2}(1 + D_6),$$

where

$$B_5 = \sqrt{4 + 2m(1-\upsilon_0) + m^2 + 4\lambda^2 - 2B_7},$$

$$B_6 = \sqrt{4 + 2m(1 - v_0) + m^2 + 4\lambda^2 + 2B_7},$$
$$B_7 = \sqrt{m^2(1 + v_0)^2 + 4\lambda^2(m + 2)(2 - mv_0)},$$
$$C_5 = \sqrt{7 + 4\lambda^2 - 2C_7}, \qquad C_6 = \sqrt{7 + 4\lambda^2 + 2C_7}, \qquad C_7 = \sqrt{1 + 24\lambda^2},$$
$$D_5 = \sqrt{3 + 4\lambda^2 - 2D_7}, \qquad D_6 = \sqrt{3 + 4\lambda^2 + 2D_7}, \qquad D_7 = \sqrt{1 + 8\lambda^2}.$$

Appendix B

Expressions of constants T_i $(i = 1, 2, \ldots, 20)$ appearing in (18)–(25) are given below.

$$T_1 = p_{ou} r_{ou}^{2+a_1} - p_{in} r_{in}^{2+a_1}, \qquad T_2 = p_{in} r_{in}^{2+a_1} r_{ou}^{2a_1} - p_{ou} r_{in}^{2a_1} r_{ou}^{2+a_1},$$
$$T_3 = -T_1((a_1 - 1)v_0 - 1)/(a_1 + 1), \qquad T_4 = -T_2((a_1 + 1)v_0 + 1)/(a_1 - 1),$$
$$T_5 = p_{ou} r_{ou}^{2-a_2} - p_{in} r_{in}^{2-a_2}, \qquad T_6 = p_{in} r_{in}^{2-a_2} r_{ou}^{a_4} - p_{ou} r_{in}^{a_4} r_{ou}^{2-a_2},$$
$$T_7 = -r_{ou}^m T_5((a_4 + m)v_0 - 2)/(a_2 + a_4 - m - 1),$$
$$T_8 = -r_{ou}^m T_6((m - a_4)v_0 - 2)/(a_2 - m - 1),$$
$$T_9 = p_{ou} r_{ou}^{a_8} - p_{in} r_{in}^{a_8}, \qquad T_{10} = p_{in} r_{in}^{a_8} r_{ou}^{\sqrt{5}} - p_{ou} r_{ou}^{a_8} r_{in}^{\sqrt{5}}, \qquad T_{11} = a_8 v_0 T_9/(a_7 - 1),$$
$$T_{12} = -r_{ou} T_9/a_7, \qquad T_{13} = a_7 v_0 T_{10}/(a_8 - 1), \qquad T_{14} = -r_{ou} T_{10}/a_8,$$
$$T_{15} = p_{ou} r_{ou}^{a_6} - p_{in} r_{in}^{a_6}, \qquad T_{16} = p_{in} r_{in}^{a_6} r_{ou}^{\sqrt{5}} - p_{ou} r_{ou}^{a_6} r_{in}^{\sqrt{5}}, \qquad T_{17} = T_{15}/(2 - a_5),$$
$$T_{18} = a_7 r_{ou} v_0 T_{15}/(1 - a_5), \qquad T_{19} = T_{16}/(2 - a_6), \qquad T_{20} = a_8 r_{ou} v_0 T_{16}/(1 - a_6).$$

References

1. Leissa, W., Vagins, M.: The design of orthotropic materials for stress optimization. Int. J. Solids Struct. **14**, 517–526 (1978)
2. Icardi, U., Ferrero, L.: Optimizing fiber direction in perforated orthotropic media to reduce stress concentration. Compos. Sci. Technol. **69**, 575–585 (2009)
3. Batra, R.C., Jin, J.: Natural frequencies of a functionally graded anisotropic rectangular plate. J. Sound Vib. **282**, 509–516 (2005)
4. Zamani, N.M., Rahimi, G.H.: Deformations and stresses in rotating FGM pressurized thick hollow cylinder under thermal load. Sci. Res. Essay **4**(3), 131–140 (2009)
5. Jin, X., Wu, L.Z., Sun, Y.G., Guo, L.C.: Microstructure and mechanical properties of ZrO2/NiCr functionally graded materials. Mater. Sci. Eng. A **509**, 63–68 (2009)
6. Lee, K.H., Lee, Y.J., Cho, S.B.: Characteristics of a transiently propagating crack in functionally graded materials. J. Mech. Sci. Technol. **23**, 1306–1322 (2009)
7. Genin, G.M., Birman, V.: Micromechanics and structural response of functionally graded, particulate-matrix, fiber-reinforced composites. Int. J. Solids Struct. **46**, 2136–2150 (2009)
8. Nemat Alla, M., Ahmed, K.I.E., Hassab Allah, I.: Elastic-plastic analysis of two-dimensional functionally graded materials under thermal loading. Int. J. Solids Struct. **46**, 2774–2786 (2009)
9. Khabbaz, R.S., Manshadi, B.D., Abedian, A.: Nonlinear analysis of FGM plates under pressure loads using the higher-order shear deformation theories. Compos. Struct. **89**, 333–344 (2009)
10. Lechnitskii, S.G.: Theory of Elasticity of an Anisotropic Body. Mir, Moscow (1981)
11. Timoshenko S, P., Goodier, J.N.: Theory of Elasticity. McGraw–Hill, New York (1969)
12. Batra, R.C.: Finite plane strain deformations of rubberlike materials. Int. J. Numer. Methods Eng. **15**(1), 145–160 (1980)

13. Pan, E., Roy, A.K.: A simple plane-strain solution for functionally graded multilayered isotropic cylinders. Struct. Eng. Mech. **24**(6), 727–740 (2006)
14. Horgan, C.O., Chan, A.M.: Pressurized hollow cylinder or disk problem for functionally graded isotropic linear elastic materials. J. Elast. **55**(1), 43–59 (1999)
15. Tarn, J.Q.: Exact solutions for functionally graded anisotropic cylinders subjected to thermal and mechanical loads. Int. J. Solids Struct. **38**, 8189–8206 (2001)
16. Jabbari, M., Sohrabpour, S., Eslami, M.R.: General solution for mechanical and thermal stresses in a functionally graded hollow cylinder due to nonaxisymmetric steady-state loads. J. Appl. Mech. **70**, 111–118 (2003)
17. Zimmerman, R.W., Lutz, M.P.: Thermal stresses and thermal expansion in a uniformly heated functionally graded cylinder. J. Therm. Stress. **22**, 177–188 (1999)
18. Oral, A., Anlas, G.: Effects of radially varying moduli on stress distribution of nonhomogeneous anisotropic cylindrical bodies. Int. J. Solids Struct. **42**(20), 5568–5588 (2005)
19. Shao, Z.S., Wang, T.J.: Three-dimensional solutions for the stress fields in functionally graded cylindrical panel with finite length and subjected to thermal/mechanical loads. Int. J. Solids Struct. **43**, 3856–3874 (2006)
20. Tarn, J.Q., Chang, H.H.: Torsion of cylindrical orthotropic elastic circular bars with radial inhomogeneity: some exact solutions and end effects. Int. J. Solids Struct. **45**, 303–319 (2008)
21. Batra, R.C.: Torsion of a functionally graded cylinder. AIAA J. **44**(6), 1363–1365 (2006)
22. Tutuncu, N.: Stresses in thick-walled FGM cylinders with exponentially-varying properties. Eng. Struct. **29**, 2032–2035 (2007)
23. Chen, Y.Z., Lin, X.Y.: Elastic analysis for thick cylinders and spherical pressure vessels made of functionally graded materials. Comput. Mater. Sci. **44**, 581–587 (2008)
24. Theotokoglou, E.E., Stampouloglou, I.H.: The radially nonhomogeneous elastic axisymmetric problem. Int. J. Solids Struct. **45**, 6535–6552 (2008)
25. Marur, P.R., Tippur, H.V.: Evaluation of mechanical properties of functionally graded materials. J. Test. Eval. **26**, 539–545 (1998)
26. Mohammadi, M., Dryden, J.R.: Influence of the spatial variation of Poisson's ratio upon the elastic field in nonhomogeneous axisymmetric bodies. Int. J. Solids Struct. **46**, 788–795 (2009)
27. Li, X.F., Peng, X.L.: A pressurized functionally graded hollow cylinder with arbitrarily varying material properties. J. Elast. **96**, 81–95 (2009)
28. Batra, R.C.: Optimal design of functionally graded incompressible linear elastic cylinders and spheres. AIAA J. **46**(8), 2050–2057 (2008)
29. Batra, R.C., Nie, G.J.: Analytical solutions for functionally graded incompressible eccentric and nonaxisymmetrically loaded circular cylinders. Compos. Struct. **92**, 1229–1245 (2010)
30. Nie, G.J., Batra, R.C.: Stress analysis and material tailoring in isotropic linear thermoelastic incompressible functionally graded rotating disks of variable thickness. Compos. Struct. **92**, 720–729 (2010)
31. Nie, G.J., Batra, R.C.: Material tailoring and analysis of functionally graded isotropic and incompressible linear elastic hollow cylinders. Compos. Struct. **92**, 265–274 (2010)
32. Batra, R.C., Iaccarino, G.L.: Exact solutions for radial deformations of functionally graded isotropic and incompressible second-order elastic cylinders. Int. J. Non-Linear Mech. **43**, 383–398 (2008)
33. Batra, R.C., Bahrami, A.: Inflation and eversion of functionally graded nonlinear elastic incompressible cylinders. Int. J. Non-Linear Mech. **44**, 311–323 (2009)
34. Chatzigeorgiou, G., Charalambakis, N., Murat, F.: Homogenization of a pressurized tube made of elastoplastic materials with discontinuous properties. Int. J. Solids Struct. **46**, 3902–3913 (2009)